

SORTING HUMAN PROSTATE EPITHELIAL (HPET) CELLS IN AN INERTIAL MICROFLUIDIC DEVICE

N. Nivedita,¹ P. V. Giridhar,² S. Kasper,² and I. Papautsky¹

¹School of Electronic and Computing Systems, University of Cincinnati, Cincinnati, OH USA

²College of Medicine, University of Cincinnati, Cincinnati, OH USA

ABSTRACT

In this work, we demonstrate continuous size-based sorting and separation of cells in a simple passive microfluidic device. Our approach takes advantage of the principles of inertial microfluidics and Dean drag forces in spiral microchannels for successful separation of HPET (human prostate epithelial) cells, obtained from a high grade (Gleason 9) prostate punch biopsy, with high throughput (~10,000cells/min) and separation efficiency (>90%). The approach can be extended to other cell types and mixtures.

KEYWORDS: Inertial microfluidics, HPET cells, Cell-sorting, Continuous flow separation

INTRODUCTION

Cell separation is critical to sample preparation and analysis involved in identification and determination of cells exhibiting stem cell characteristics. For example, reconstitution of the original Human Prostate cancer specimen from the epithelial cell line of the prostate (HPET) signifies the role of stem cells in cancer growth [1]. The HPET cancer stem cell model is crucial to investigate the mechanisms by which cancer stem cells (CSCs) promote metastasis and the emergence of treatment-resistant prostate cancer. Hence, separation of HPET cells is critical to identification of stem/tumor cells from prostate tissue biopsies. The only way to sort these cells is flow cytometry, which yields low to no viability due to the fragility of these cells.

Inertial microfluidics offers ability for size-based separation of cells at low cost and high efficiency. The spiral inertial microfluidic devices we introduced recently [2,3] achieve continuous size-based separation of cell mixtures with high throughput. Due to parabolic velocity profile in a plane Poiseuille flow, the shear gradient induces inertial lift forces (F_{IL}) on the neutrally buoyant cells (or microparticles), causing them to migrate towards the channel walls. However, as they migrate closer to the channel walls they are repelled towards the center due to wall induced lift forces (F_{WL}). This is illustrated in Fig.1a. The net lift force (F_L) equilibrates the cells around the channel periphery in four positions at wall centerlines [2], and is given by

$$F_L = \frac{2\rho U_a^2 a_p^4}{L_c^2} \quad (1)$$

where ρ is the fluid density, a_p is the cell (or particle) diameter, U_a is the average flow velocity and L_c is the characteristic length or the hydraulic diameter. Thus, the lift force exhibits a strong dependence on cell size.

In a spiral microchannel, the centrifugal acceleration component due to the curvilinear geometry leads to formation of two counter rotating and symmetric vortices in the top and bottom half of the channel (Fig. 1). These vortices (also called Dean vortices) exert Dean force (F_D) on cells, and hence the focusing positions are reduced to a single position where the hydrodynamic forces balance the Dean drag [3]. The Dean force is given by

$$F_D = 5.4 \times 10^{-4} \pi \mu De^{1.63} a_p \quad (2)$$

where De is the dimensionless Dean number. Thus, the ratio of these forces is strongly dependent on cell/particle size (a_p^3).

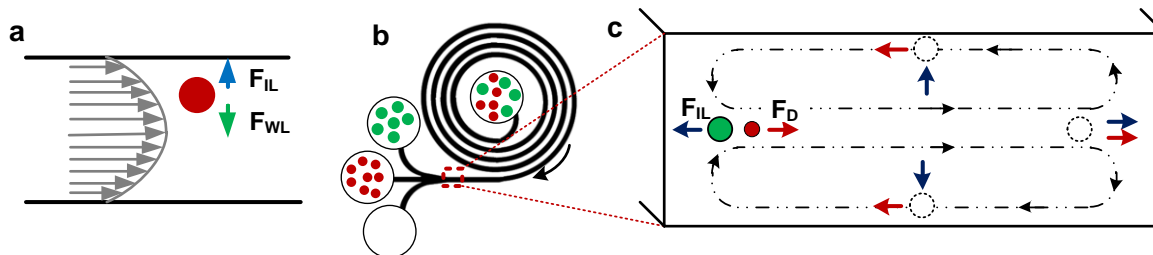


Figure 1. (a) Hydrodynamic forces, namely shear-induced inertial lift (F_{IL}) and wall-induced lift (F_{WL}), act on particles and cells in laminar flow causing them to focus along channel perimeter. (b) In a spiral microchannel, larger cells focus closer to the inner channel wall due to the balance of the hydrodynamic lift forces and Dean drag (F_D), which disrupts the equilibrium except near the inner wall (c).

METHODS

For separation, we used a single input Archimedean spiral with 2mm inner radius and $500\mu\text{m} \times 100\mu\text{m}$ channel cross-section. Previous spiral designs had a focusing length of 40cm with an inner radius of 1cm which made the device quite large [3]. To optimize the device, we used the Archimedean spiral equation

$$r = a + b\theta \quad (3)$$

where r and θ are polar coordinates, and a, b are parametric real numbers. The focusing length can be calculated as

$$L_F = \frac{U_a}{U_D} L_M \quad (4)$$

where L_F is the minimum focusing length at a particular dean number with U_D as the dean velocity and U_a as the average flow velocity and L_M , the Dean migration length.

Fig. 2 illustrates variation of the Dean number and residual with respect to the downstream length, indicating the optimal focusing length. It is apparent that the Dean number decreases with the downstream length while maintaining the dean vortices required for focusing the particles/cells. For the device in this work, the optimized focusing length was determined to be $\sim 8\text{cm}$ (6-loops).

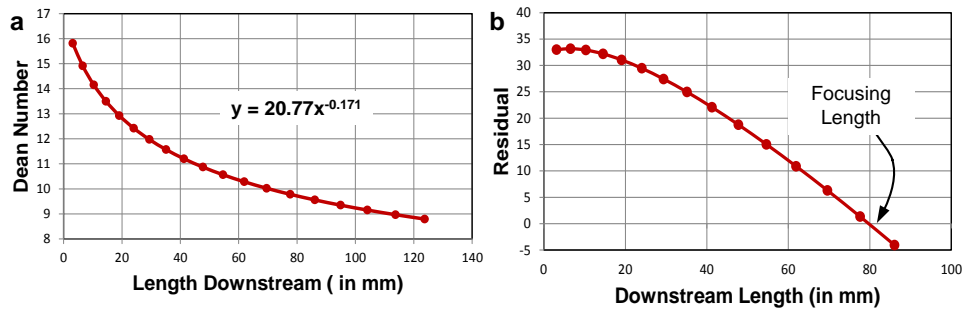


Figure 2. Change in (a) Dean number and (b) residual with the downstream length in the spiral channel with initial radius of 2mm and the focusing length $\sim 8\text{cm}$

After optimization, standard soft lithography PDMS process was used to fabricate the devices (Fig. 3a). We used a four outlet system for the optimized Archimedean spiral device. To confirm the focusing length, we ran $20\mu\text{m}$ polystyrene particles through the device and observed the focusing position with regards to the inner channel wall (Fig. 3a). The flow parameters were optimized using fluorescently-labeled polystyrene particles $\sim 10, 15$ and $20\mu\text{m}$ in diameter, satisfying the diameter to characteristic length ratio $a_p/L_C > 0.07$ criterion [3]. These particle sizes were used since the HPET cells were measured to be $11\text{-}23\mu\text{m}$.

RESULTS AND DISCUSSION

We initially characterized our devices and confirmed their operation using neutrally-buoyant fluorescently-labeled polystyrene particles. In accordance with previous observations [3], the larger particles ($20\mu\text{m}$) focused closer to the inner

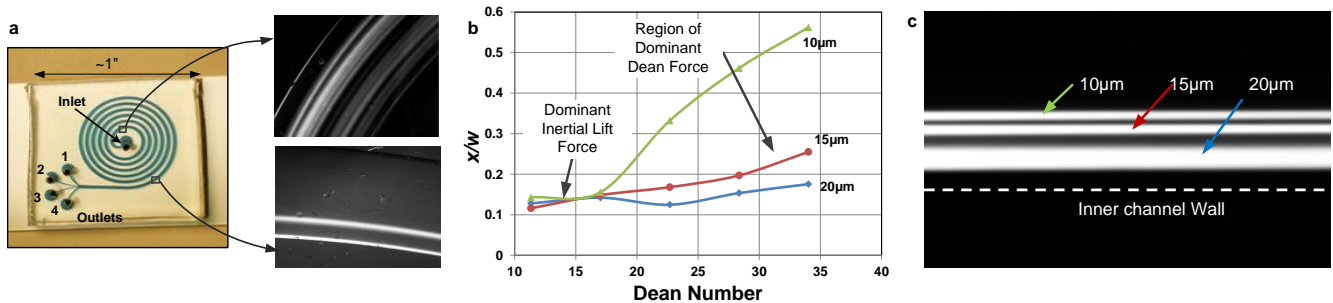


Figure 3. (a) Fabricated 6-loop spiral device and the fluorescent images illustrating the distribution of $20\mu\text{m}$ particles in the channel at the inlet (unfocused) and the outlet (focused stream). (b) Normalized focusing position of particles (x is the distance of the focused stream from the inner channel wall, and w is the width of the channel) as function of Dean number. (c) Fluorescent image of the focused streams of all three particles.

channel wall due to the stronger inertial lift force acting on them. As the particle size reduced, the Dean force begins to dominate. Thus, particles with smaller diameter ($\sim 10\mu\text{m}$) focused away from the inner channel wall and towards the center of the channel. Fig. 3b indicates the normalized position of focused particles as a function of Dean number, permitting selection of optimal flow parameters for separation. These results clearly show that the equilibrium position of the focused cells is strongly dependent on their size, as well as flow properties and channel geometry. This is also demonstrated in Fig. 3c, which illustrated focused streams of all three particles.

The HPET cells were successfully sorted and separated at a flow rate of $\sim 2\text{mL}/\text{min}$. Fig.4a shows the fluorescent image of the focused streams of HPET cells (11-23 μm) within the range of 10, 15 and 20 μm . The larger HPET cells ($>20\mu\text{m}$ diameter) eluted in the first outlet closest to the channel inner wall. The smaller cells ($\sim 15\mu\text{m}$) eluted in the second outlet, and the smallest $\sim 10\mu\text{m}$ cells eluted in the third outlet from the inner wall (Fig.4).

Because these cells are highly fragile, the flow rate was optimized to prevent them from lysing in the device, leading to $\sim 100\%$ viability at the output with a throughput of 10,000cells/min. These devices were also used to separate other cell lines, including DU-145 (derived from brain metastasis) and LNCaP (derived from left supraclavicular lymph node), from HPET cells (Fig. 4d).

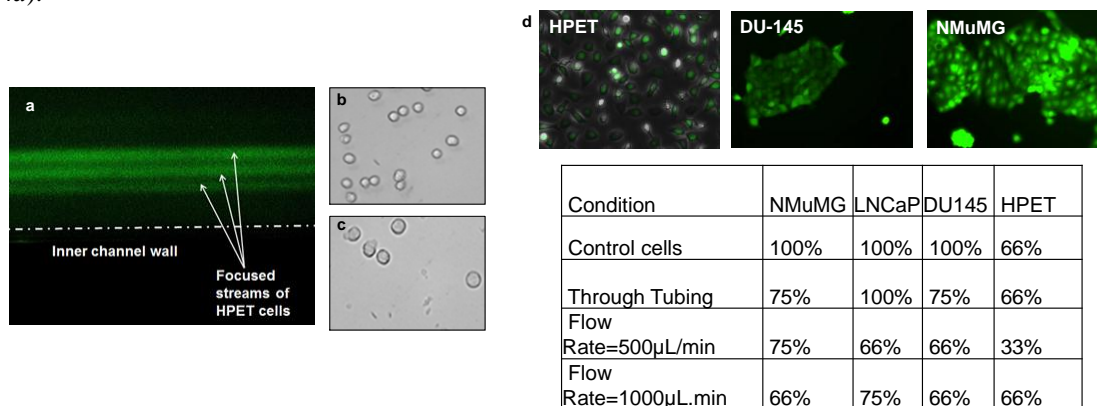


Figure 4. (a) Fluorescent image of the focused streams of HPET cells. Phase contrast images of HPET cells at outlets 2&3 (b) and outlet1 (c). (d) Images of fluorescently labeled NMuMG, LNCaP, DU-145 and HPET cells (3mM CMFDA dye) with the viability of cells in various conditions.

CONCLUSION

This work described the use of a simple 6-loop Archimedean spiral for continuous size-based sorting of HPET cells. It is the first demonstration of separation of HPET cells with high viability ($>90\%$) and throughput of 10,000cell/min. This system not only boasts smaller area (smaller focusing length), but higher cell viability and higher efficiency as compared to the previous spiral design [3]. The described approach is broadly applicable, and could be extended to other cell types and cell sizes. The simple planar structure of the device and the passive mechanism of separation make these disposable devices an easy-to-use tool for cell biologists and gives way to the possible development of sample preparation and analysis system on a chip.

ACKNOWLEDGEMENTS

This work was partially supported by a grant from the National Institute of Diabetes and Digestive and Kidney Diseases (NIDDK, R01DK060957)..

REFERENCES

- [1] G. Gu, J. Yuan, M. Wills, and S. Kasper, *J. Cell Sci.*, **114**, 3865-3872, 2001.
- [2] A. A. S. Bhagat, S. S. Kuntaegowdanahalli, and I. Papautsky, *Microfluid. Nanofluid.*, **7**, 217-226, 2009.
- [3] S. S. Kuntaegowdanahalli, A. A. S. Bhagat, and I. Papautsky, *Lab Chip*, **9**, 2973-2980, 2009.
- [4] S. Kasper, *J. Cell. Physiol.* **216**, 332-336, 2008.

CONTACT

*I. Papautsky, tel: +1-513-2347; ian.papautsky@uc.edu